Finally, it is interesting as to whether 16q-linked ADCA and SCA4 are allelic or not [26]. Since the possible pyramidal tract signs with cerebellar ataxia seen in our patients are common in 16q-linked ADCA and SCA4 despite the absence of sensory axonal neuropathy in the former, the two disorders might be allelic. There is a possibility that patients with 16q-linked ADCA will hereafter be found throughout the world. Further investigations are necessary to clarify the molecular mechanisms underlying 16q-linked ADCA and SCA4.

Acknowledgements

The authors thank the families that participated in this study. This work was supported by a grant from the Research Committee for Ataxic Diseases (Y.T.) of the Ministry of Health, Labor and Welfare, Japan.

References

[1] Harding AE. The clinical features and classification of the late onset autosomal dominant cerebellar ataxias: a study of 11 families, including descendants of "Drew family of Walworth". Brain 1982; 105:1–28.
[2] Manto MU. The wide spectrum of spinocerebellar ataxias (SCAs). Cerebellum 2005;4:2–6.
[3] Cagnoli C, Mariotti C, Taroni F, Seri M, Brussino A, Michielotto C, et al. SCA28, a novel form of autosomal dominant cerebellar ataxia on chromosome 18p11.22-q11.2. Brain 2006;129:235–42.
[4] Flanigan K, Gardner K, Alderson K, Galster B, Otterud B, Leppert MF, et al. Autosomal dominant spinocerebellar ataxia with sensory axonal neuropathy (SCA4): clinical description and genetic localization to chromosome 16q22.1. Am J Hum Genet 1996;59:392–9.
[5] Hellenbroich Y, Bubel S, Pawlack H, Opitz S, Vieregge P, Schwinger E, et al. Refinement of the spinocerebellar ataxia type 4 locus in a large German family and exclusion of CAG repeat expansions in this region. J Neurol 2003;250:668–71.
[6] Nagaoka U, Takashima M, Ishikawa K, Yoshizawa K, Yoshizawa T, Ishikawa M, et al. A gene on SCA4 locus causes dominantly inherited pure cerebellar ataxia. Neurology 2000;54:1971–5.
[7] Li M, Ishikawa K, Toru S, Tomimitsu H, Takashima M, Goto J, et al. Physical map and haplotype analysis of 16q-linked autosomal dominant cerebellar ataxia (ADCA) type III in Japan. J Hum Genet 2003;48:111–8.
[8] Ishikawa K, Tanaka H, Saito M, Ohkoshi N, Fujita T, Yoshizawa K, et al. Japanese families with autosomal dominant pure cerebellar ataxia map to chromosome 19p13.1-13.2 and are strongly associated with mild CAG expansions in the spinocerebellar ataxia type 6 gene in chromosome 19p13.1. Am J Hum Genet 1997;61:336–46.
[9] Ishikawa K, Toru S, Tsunemi T, Li M, Kobayashi K, Yokota T, et al. An autosomal dominant cerebellar ataxia linked to chromosome 16q22.1 is associated with a single-nucleotide substitution in the 5′ untranslated region of the gene encoding a protein with spectrin repeat and Rho guanine-nucleotide exchange-factor domains. Am J Hum Genet 2005;77:280–96.
[10] Owada K, Ishikawa K, Toru S, Ishida G, Gomyoda M, Tao O, et al. A clinical, genetic, and neuropathologic study in a family with 16q-linked ADCA type III. Neurology 2005;65:629–32.
[11] Namekawa M, Takiyama Y, Ando Y, Sakoe K, Muramatsu S, Fujimoto K, et al. Choreiform movements in spinocerebellar ataxia type 1. J Neurol Sci 2001;187:103–6.
[12] Sanpei K, Takano H, Igarashi S, Sato T, Oyake M, Sasaki H, et al. Identification of the spinocerebellar ataxia type 2 gene using a direct identification of repeat expansion and cloning technique, DIRECT. Nat Genet 1996;14:277–84.
[13] Takiyama Y, Igarashi S, Rogaeva EA, Endo K, Rogaev EI, Tanaka H, et al. Evidence for inter-generational instability in the CAG repeat in the MJD1 gene and for conserved haplotypes at flanking markers amongst Japanese and Caucasian subjects with Machado-Joseph disease. Hum Mol Genet 1995;4:1137–46.
[14] Takiyama Y, Sakoe K, Namekawa M, Soutome M, Esumi E, Ogawa T, et al. A Japanese family with spinocerebellar ataxia type 6 which includes 3 individuals homozygous for an expanded CAG repeat in the SCA6/CACNL1A4 gene. J Neurol Sci 1998;158:141–7.
[15] David G, Abbas N, Stevanin G, Durr A, Yvert G, Cancel G, et al. Cloning of the SCA7 gene reveals a highly unstable CAG repeat expansion. Nat Genet 1997;17:65–70.
[16] Hokezu Y, Takiyama Y, Sakoe K, Nagamatsu K. A familial case of spinocerebellar ataxia type 8: its clinical findings and an issue about the genetic basis. Rinsho Shinkeigaku 2000;40:1116–21 [in Japanese].
[17] Holmes SE, O'Hearn EE, McInnis MG, Gorelick-Feldman DA, Kleiderlein JJ, Callahan C, et al. Expansion of a CAG trinucleotide repeat in the 5′ region of PPP2R2B is associated with SCA12. Nat Genet 1999;23:391–2.
[18] Nakamura K, Jeong SY, Uchihara T, Anno T, Nagashima K, Nagashima T, et al. SCA17, a novel autosomal dominant cerebellar ataxia caused by an expanded polyglutamine in TATA-binding protein. Hum Mol Genet 2001;10:1441–8.
[19] Takiyama Y, Sakoe K, Amaike M, Soutome M, Ogawa T, Nakano I, et al. Single sperm analysis of the CAG repeats in the gene for dentatorubral-pallidoluysian atrophy (DRPLA): the instability of the CAG repeats in the DRPLA gene is prominent among the CAG repeat diseases. Hum Mol Genet 1999;8:453–7.
[20] Hirano R, Takashima H, Okubo R, Tajima K, Okamoto Y, Ishida S, et al. Fine mapping of 16q-linked autosomal dominant cerebellar ataxia type III in Japanese families. Neurogenetics 2004;5:215–21.
[21] Shimizu Y, Yoshida K, Okano T, Ohara S, Hashimoto T, Fukushima Y, et al. Regional features of autosomal-dominant cerebellar ataxia in Nagano: clinical and molecular genetic analysis of 86 families. J Hum Genet 2004;49:610–6.
[22] Ikeuchi T, Takano H, Koide R, Horikawa Y, Honma Y, Onishi Y, et al. Spinocerebellar ataxia type 6: CAG repeat expansion in (1A-voltage-dependent calcium channel gene and clinical variations in Japanese population. Ann Neurol 1997;42:879–84.
[23] Geschwind DH, Perlman S, Figueroa KP, Karrim J, Baloh RW, Pulst SM. Spinocerebellar ataxia type 6: frequency of the mutation and genotype-phenotype correlations. Neurology 1997;49:1247–51.
[24] Takahashi H, Ishikawa K, Tsutsumi T, Fujigasaki H, Kawata A, Okiyama R, et al. A clinical and genetic study in a large cohort of patients with spinocerebellar ataxia type 6. J Hum Genet 2004; 49:256–64.
[25] Sasaki H, Yabe I, Tashiro K. The hereditary spinocerebellar ataxias in Japan. Cytogenet Genome Res 2003;100:198–205.
[26] Hellenbroich Y, Pawlack H, Rub U, Schwinger E, Zuhlke C. Spinocerebellar ataxia type 4; investigation of 34 candidate genes. J Neurol 2005;252:1472–5.

Limited Wegener's Granulomatosis Manifested by Abducens Nerve Palsy Resulting From Pachymeningitis

Takeshi Kamimura, MD,‡ Haruo Shimazaki, MD,† Mitsuya Morita, MD,† Imaharu Nakano, MD,† Hitoaki Okazaki, MD,‡ and Seiji Minota, MD‡*

A 50-year-old man was referred to our hospital on April 30, 2002, presenting with rightsided headache associated with paralysis of the right abducens nerve for several days. As a recent history, he had a rightsided acute anterior uveitis, otitis media, chronic sinusitis, and intranasal tumor. Laboratory examination disclosed an elevated erythrocyte sedimentation rate (66 mm/h; normal, <10 mm/h) and proteinase 3 antineutrophil cytoplasmic antibody (ANCA) (36 EU; normal, <10 EU). Urinalysis was normal. Cerebrospinal fluid analysis revealed a slightly increased white cell count at 10 cells in 3 visual fields dominated by mononuclear cells and an elevated level of protein at 91 mg/dL. Chest X-ray examination demonstrated no significant abnormality. Gadolinium-enhanced brain magnetic resonance imaging (MRI) showed pachymeningeal enhancements over the right frontal convexities, cavernous sinus, cerebellar tentorium, and skull base (Fig. 1A, C, E). Histologic confirmation by biopsy of intranasal tumor or pachymeninges was not performed because of the patient's refusal. He was diagnosed clinically with limited Wegener's granulomatosis (WG) complicated by abducens nerve palsy resulting from pachymeningitis. Thirty milligrams per day of prednisone was initiated with an improvement of the symptoms, laboratory data, and MRI findings (Fig. 1B, D, F).

From the *Department of Medicine, Utsunomiya Social Insurance Hospital, Minamitakasago-chou, Utsunomiya-city, Tochigi, Japan; and the Divisions of †Neurology and ‡Rheumatology & Clinical Immunology, Department of Medicine, Jichi Medical School, Minamikawachi-machi, Kawachi-gun, Tochigi, Japan.

Reprints: Takeshi Kamimura, MD, Division of Rheumatology & Clinical Immunology, Department of Medicine, Jichi Medical School, 3311-1 Yakushiji, Minamikawachi-machi, Kawachi-gun, Tochigi, Japan. E-mail: kamiken@ms2.jichi.ac.jp

ISSN: 1076-1608/06/1205-0259
DOI: 10.1097/01.rhu.0000239904.62352.5e

DISCUSSION

Involvement of the central nervous system in patients with WG occurs in 8%, and it is quite rare that such an involvement was found at the time of diagnosis.[1] Recently, pachymeningitis has been reported as a neurologic manifestation of ANCA-related vasculitis.[2]

Fam et al reviewed 15 cases of WG with biopsy-proven pachymeningitis and found some similarities they shared, including its early occurrence in the course of active and limited WG, an elevated erythrocyte sedimentation rate, severe headache and cranial neuropathies in the absence of nuchal rigidity, cerebrospinal fluid findings with mild lymphocytic pleocytosis and elevated protein concentration, a positive serum ANCA, detection of pachymeningitis by gadolinium-enhanced brain MRI, and a favorable response to the treatment with prednisone.[2] The findings of the present case were quite similar to these features. Based on these findings, he was given a diagnosis of WG clinically.

In conclusion, pachymeningitis must be taken into consideration when a patient with WG has a headache and cranial neuropathy. Gadolinium-enhanced MRI is quite useful not only for the diagnosis, but also the follow up of pachymeningitis. Heightened awareness, early diagnosis, and timely therapy for this atypical presentation of WG are important to prevent permanent neurologic dysfunction and further disease progression.[2]

REFERENCES

1. Stone JH, Hoffman GS. Wegener's granulomatosis and lymphomatoid granulomatosis. In: Hochberg MC, Silman AJ, eds. *Rheumatology,* vol 2, 3rd ed. London: Mosby; 2003:1635–1648.
2. Fam AG, Lavine E, Lee L, et al. Cranial pachymeningitis: an unusual manifestation of Wegener's granulomatosis. *J Rheumatol.* 2003;30:2070–2074.

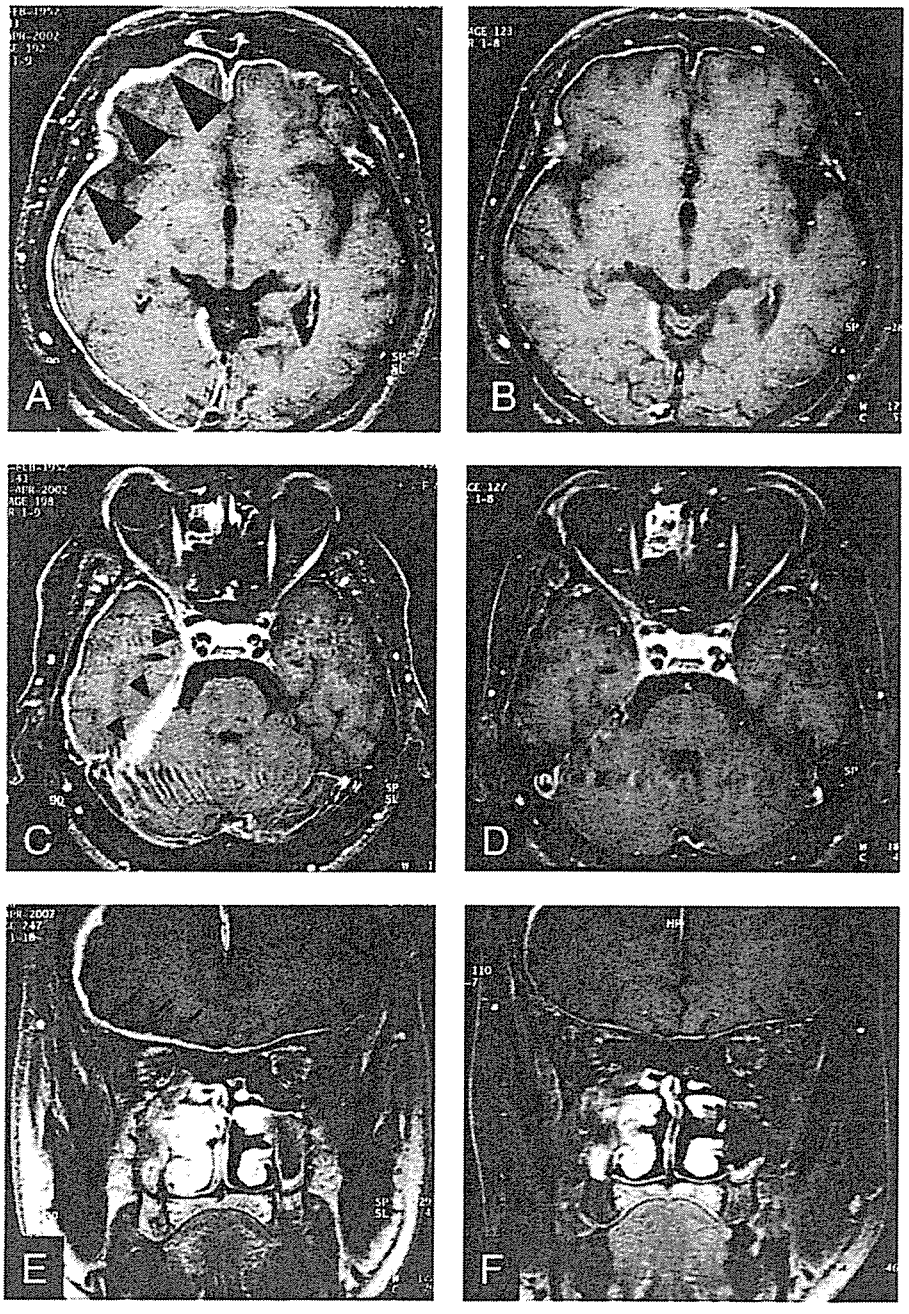

FIGURE 1. Gadolinium-enhanced T1-weighted brain magnetic resonance image on admission (**A**, **C**, and **E**) and 4 weeks after treatment with corticosteroid (**B**, **D**, and **F**). Axial scan showing pachymeningeal enhancement over the right frontal convexities (**A**, big arrowheads), cavernous sinus, and cerebellar tentorium (**C**, small arrowheads). Coronal scan showing pachymeningeal enhancement along the skull base (**E**, arrows). All the enhanced lesions were improved with corticosteroid (**B**, **D**, and **F**). **A–D**, axial views; **E** and **F**, coronal views.

Neuropathology 2006; **26**, 433–437 doi:10.1111/j.1440-1789.2006.00705.x

Case Report

Severe cortical involvement in MV2 Creutzfeldt–Jakob disease: An autopsy case report

Kenji Ishihara,[1,2] Masayuki Sugie,[1] Jun-ichi Shiota,[1,2] Mitsuru Kawamura,[1] Tetsuyuki Kitamoto[3] and Imaharu Nakano[4]

[1]Department of Neurology, Showa University School of Medicine, Tokyo, [2]Department of Neurology, Ushioda General Hospital, Kanagawa, [3]Department of Neurological Science, Tohoku University Graduate School of Medicine, Sendai, and [4]Department of Neurology, Jichi Medical School, Tochigi, Japan

MV2 type sporadic Creutzfeldt–Jakob disease (sCJD) is reported to have a long duration and marked involvement of the cerebral deep gray matter. We describe an autopsied long-surviving sCJD case of MV2. In the early stages, the patient exhibited memory impairment, attention deficit and semantic memory disorder. Diffusion-weighted MRI showed abnormal hyperintensity signals along the cerebral cortex, sparing the thalami and basal ganglia. Pathological observations included: severe spongiosis throughout the cerebral cortex, several kuru plaques and plaque-like PrP deposits in the cerebellum, with only minimal degeneration in the thalami and basal ganglia. Our case suggests that MV2 has a wide clinicopathological spectrum, which ranges from "VV2" to "MM2" type.

Key words: Creutzfeldt–Jakob disease, MRI, MV2, pathology.

INTRODUCTION

Cases of sporadic Creutzfeldt–Jakob disease (sCJD) present with a variety of symptoms and courses. In 1999, Parchi *et al.* proposed a classification of sCJD based on molecular and phenotypic features of 300 cases, using a combination of two factors: polymorphic codon 129 of the prion protein gene, that is, methionine homozygote (MM), heterozygote (MV) or valine homozygote (VV); and the physicochemical properties of protease-resistant prion protein (PrP) accumulated in the brain, i.e. type 1 or type 2.[1] Most cases of classical sCJD are MM1 or MV1. In this classification, MV2 cases present with a long clinical illness, ataxia and cognitive impairment in the initial stage, and characteristic kuru-plaques in the cerebellum.

Here, we report a case of MV2 type sCJD presenting with atypical pathological findings.

CLINICAL SUMMARY

Case report

A 73-year-old woman was brought to our hospital by her daughters because of 6-month history of forgetfulness and abnormal behavior. She could not recall the names of her acquaintances or daily objects and used pronouns frequently because she was unable to remember the names of persons or things to which she was referring. She could feed and dress herself. Her family had no history of neurological disease. She had had a brainstem hemorrhage (right pontine base) at age 66. She had never undergone neurosurgery involving a dura mater graft, deep brain electrodes or corneal transplantation.

On admission, she was oriented to date and place, was polite and showed no antisocial or disinhibitory behavior. She showed attention deficit and semantic memory disorder. On the revised edition of the Wechsler adult intelligence scale she scored verbal IQ score of 57, performance IQ score of 61, and full-scale IQ score of 56. Her cranial nerves were unremarkable, aside from palatal myoclonus and left-sided facial sensory loss. Her visual field showed no deficiency or visual extinction. The muscle tone was slightly spastic in her left upper and lower extremities. As a result of involuntary movement, such as pseudoathethosis and hyperkinesie volitionelle, her coordination was disturbed in left upper and lower extremities. She could walk using a cane in the right hand. She had sensory disturbance in all modalities on the left side of the body. These motor

Correspondence: Kenji Ishihara, MD, Department of Neurology, Showa University School of Medicine, Hatanodai 1-5-8, Shinagawa-ku, Tokyo 142-8666, Japan. Email: k-ishihara@mvj.biglobe.ne.jp

Received 14 November 2005; revised and accepted 26 December 2005.

and sensory symptoms were sequelae of the right pontine hemorrhage.

Her laboratory findings were within the normal range, including tests for syphilis, thyroid function and vitamins. The examination of cerebrospinal fluid was normal aside from a slightly elevated protein concentration (61 mg/dL). An assay of 14-3-3 protein was equivocal. An analysis of the prion protein gene showed no mutation. She had the methionine and valine heterozygote alleles for codon 129.

Brain MRI revealed hyperintense signals along the parieto-occipital lobe cortex, predominant on the left side, in the diffusion-weighted and fluid attenuated inversion recovery (FLAIR) images (Fig. 1). No abnormal finding was detected in the basal ganglia and thalami. In the T_2-weighted images, there was a high-signal lesion located at the right inferior olivary nucleus and right central tegmental tract, suggesting an old vascular disorder. The EEG showed almost symmetrical diffuse slow alpha activity and did not show periodic sharp wave complexes (PSWC).

Her condition gradually worsened, leaving her bedridden and requiring total parental nutrition within 6 months of admission. At this time, she developed myoclonus in the right upper extremity. A second assay for 14-3-3 protein in the cerebrospinal fluid was positive. Her speech output gradually decreased, but she could respond to an examiner's speech by nodding, shaking head, or speaking simple words, such as "yes" or "good morning". The EEG did not reveal typical PSWC.

About 6 months before her death, she developed complete akinetic mutism. She died of acute cardiac failure after about 4 years after her family first noticed her memory impairment. The clinical diagnosis was atypical sCJD of long duration.

Pathological findings

Histological examination of only the brain was performed. Sections from the brain were stained with HE, Klüver-Barrera, Bodian's, and PAS stains. Immunohistochemistry was performed with a monoclonal antibody 3F4 (Senetek, Maryland Heights, MO; 1:500), which recognizes the human prion protein residues 109–112, as previously described.[2]

The fixed brain weighed 960 g. Macroscopically, the brain was markedly atrophic, especially in the frontal lobe. Serial coronal sections of the cerebrum showed dilatations of the lateral and third ventricles, volume loss in the white matter, and brown pigmentation in the medial portion of the hippocampi. Serial horizontal sections of the brainstem showed linear pigmentation along the right medial leminis-

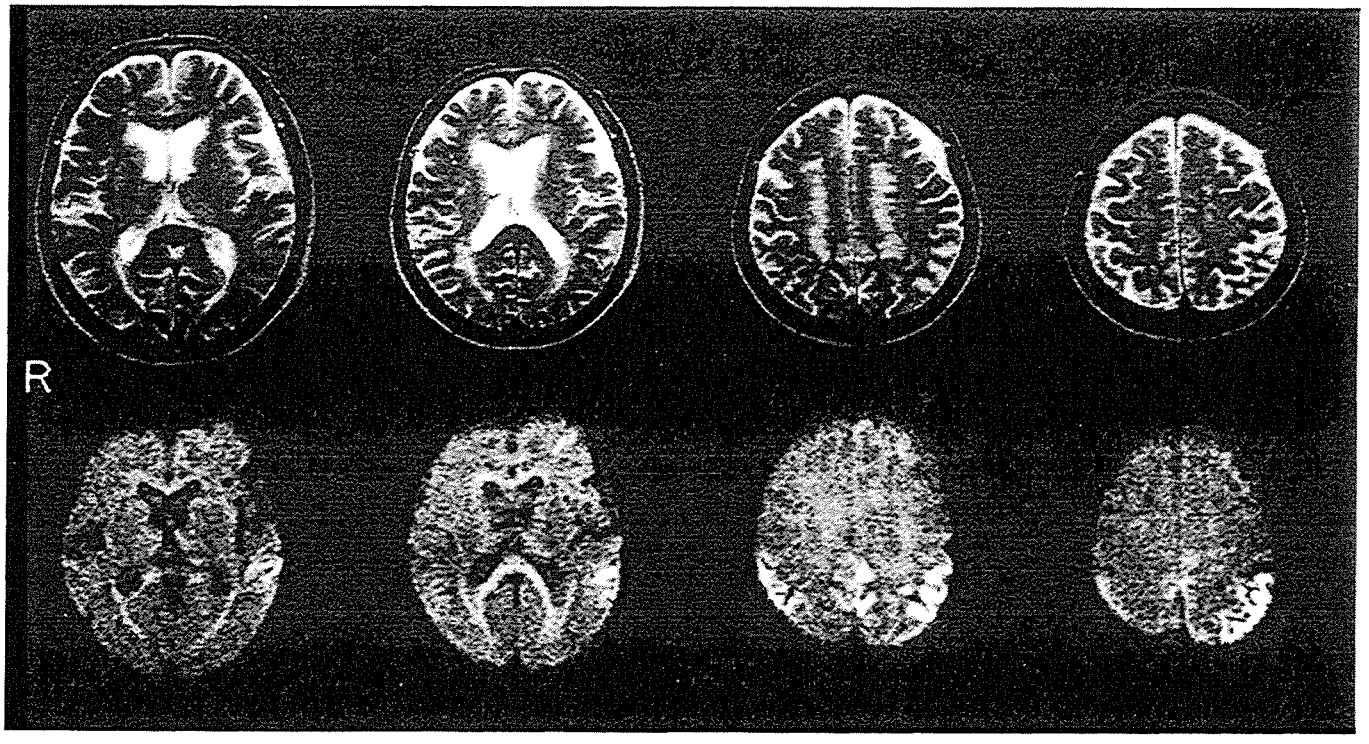

Fig. 1 MRI performed 6 months after the emergence of symptoms. An abnormally high signal is seen along the parieto-occipital lobe cortex, predominant on the left side. In the basal ganglia and thalami, no abnormal findings are seen. T_2 (upper row) and diffusion (lower row) weighted images.

cus at the pons and discoloration in the right inferior olivary nucleus. These changes were suggestive of the old pontine hemorrhage.

Diffuse spongiform change was observed throughout the cerebral cortex, including the cingulate gyrus, except for the hippocampus and subiculum (Fig. 2A). All layers showed moderate to severe status spongiosis with a tendency to spare the middle layers, giving the appearance of laminar involvement, especially around the calcarine fissure. There was moderate neuronal loss in the affected areas, but mild reactive astrocytosis only. Immunohistological staining using anti-PrP showed cortical coarse perivacuolar (Fig. 2B) and dot-like PrP deposits.

In the basal ganglia and thalami, only mild neuronal loss and mild spongiform change were observed (Fig. 2C,D). The subcortical white matter was unremarkable. Dot-like synaptic deposits of PrP were observed in the basal ganglia and thalami.

In the cerebellum, a severe loss of Purkinje cells and proliferation of Bergmann's glia were observed in the hemisphere and upper vermis (Fig. 2E). Several kuru-plaques were observed by HE and PAS staining (Fig. 2F). Many plaque-like PrP deposits were observed, especially in the upper vermis (Fig. 2G).

In the right pontine tegmentum, an irregular, old necrotic lesion, with a few macrophages containing free melanin, was observed. In the right inferior olivary nucleus, severe neuronal loss and glial proliferation, with a few vacuolated neurons, were observed, suggesting pseudohypertrophy.

Western blot analysis

Brain tissue from the right frontal lobe was homogenized, and Western blot analysis of proteinase K-resistant prion protein was performed using prion protein monoclonal antibody 3F4, as previously described.[3] In this case, type 2 prion protein was detected (Fig. 3).

DISCUSSION

Clinically, MV2 sCJD has a long course, producing cognitive impairment and ataxia initially.[1] Our case had a long clinical illness (more than 3 years from the onset of the initial symptoms to akinetic mutism) and cognitive impairment in the early stage, which is clinically compatible with MV2, with the exception of a lack of ataxia in the initial stage.

In MV2 sCJD, high signals in the basal ganglia and thalami are frequently seen on MRI T2-weighted images.[4,5] Our case exhibited abnormal hyperintensity along the cerebral cortex, but not in the basal ganglia and thalami, on MRI diffusion-weighted and FLAIR images. These image features are unusual for MV2 sCJD.

The combination of cortical hyperintensity signals on diffusion-weighted MRI, late-onset and slowly progressive dementia, and elevated levels of CSF 14-3-3 protein are characteristic findings in clinical MM2 cortical type sCJD.[6] Together with the lack of ataxia in the initial stage, our case mimicked cortical type MM2 clinically.

Neuropathologically, our case had unique findings. So far, all reported cases of MV2 sCJD show severe involvement of the cerebral subcortical nuclei and kuru-plaques and plaque-like PrP deposits in the cerebellum.[1] The degree of cerebral cortical lesions varies with the disease duration, with a tendency toward marked sponginess limited to the entorhinal cortices and deep layer of the neocortex. Cerebellar pathology is less severe, compared with the VV2 cases with similar disease duration. By contrast, our case had only mild involvement of the basal ganglia and thalami, while the entire neocortex showed marked status spongiosis, and severe loss of the Purkinje cells were observed in the cerebellum. Although kuru-plaques and plaque-like PrP deposits, observed in our case, are consistent with the pathology of MV2 sCJD, these other pathological findings are quite atypical for this type of sCJD (Table 1).

Our intensive literature search failed to find a report of MV2 sCJD with clinicopathological features similar to ours. Only one clinicopathological study of MV2 sCJD with cortical involvement in diffusion-weighted MRI has been reported.[7] However, this case showed abnormal hyperintensity signals in the basal ganglia and thalami other than the cerebral cortex, and pathological findings were restricted to the right frontal lobe cortex.

Pathologically atypical features for MV2, observed in our case, are severe extensive cortical sponginess, only mild changes in the basal ganglia and thalami and severe cerebellar pathology. Although kuru plaques, the pathological hallmarks of MV2, were also observed in our case, the cortical coarse perivacuolar PrP deposits, observed in our case, are always observed in MM2 cortical type. Plaque-like PrP deposits are always observed not only in MV2 but also in VV2.[1] Therefore, our case might have the combination of pathological features; i.e. both MM2 cortical type and VV2, besides typical MV2 features (Table 1).

In cases of MV2, valine is a candidate as the determinant factor of type 2 PrP, because most cases of MV2 show many plaque-like PrP deposits, as in VV2 cases.[1] Theoretically, methionine may also be the determinant factor of type 2 PrP. Our case suggests that MV2 has a wide clinicopathological spectrum, which ranges from "VV2 (or cerebellar)" to "MM2 (or cortical)" type. Further detailed pathological study of MV2 cases is required to justify this hypothesis.

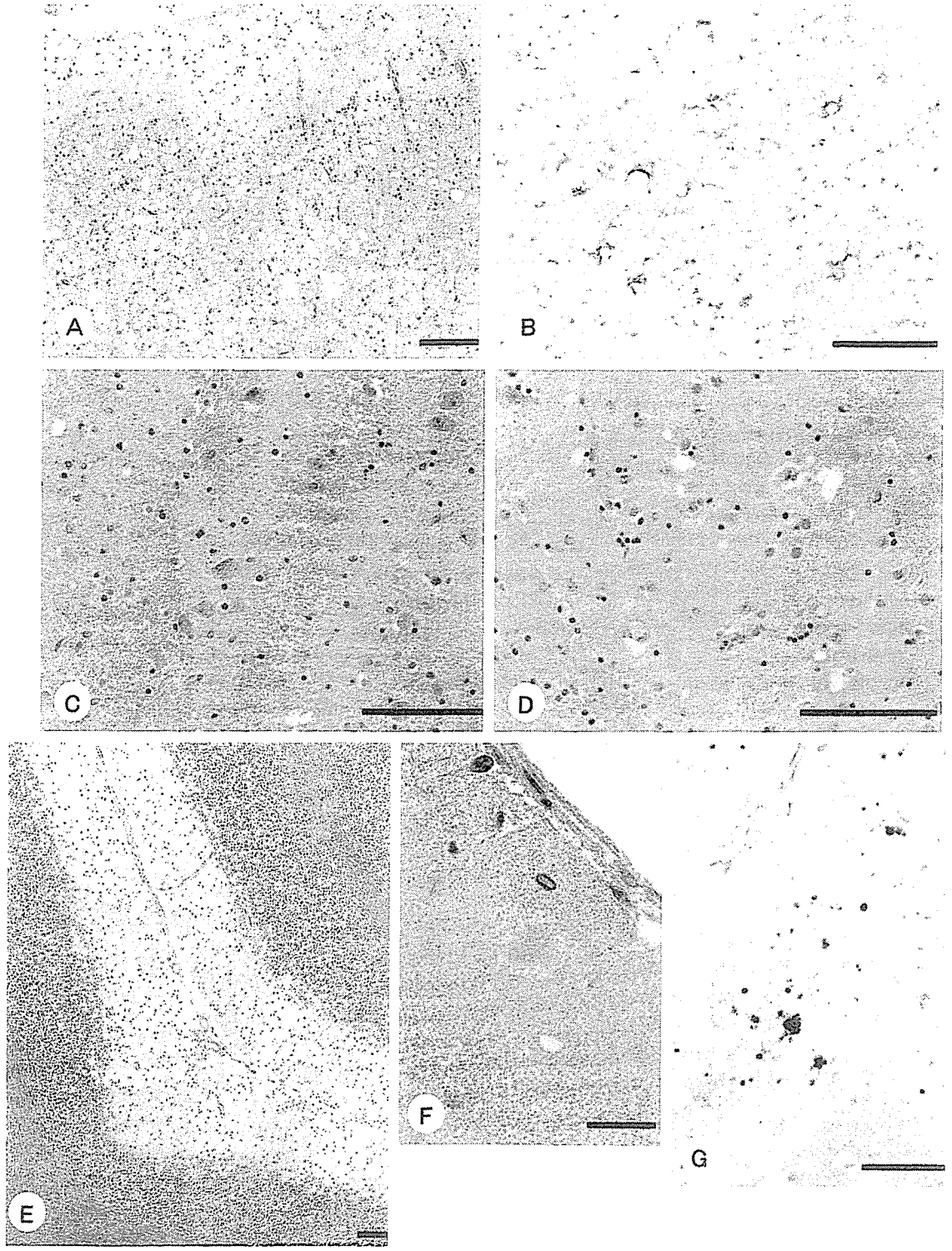

Fig. 2 Pathological findings. (A) Severe status spongiosis is observed in the left temporal lobe cortex (HE stained; scale bar = 50 μm). (B) Perivacuolar prion protein deposits are seen in the right temporal lobe cortex (immunostaining with anti-PrP antibody; scale bar = 50 μm). (C) Mild glial proliferation is seen in the left thalamus (HE stained; scale bar = 50 μm). (D) Sparse vacuolation is seen in the left putamen (HE stained; scale bar = 50 μm). (E) Severe loss of Purkinje cells and proliferation of Bergmann's glia are seen in the cerebellum (Klüver-Barrera stained; scale bar = 50 μm). (F) A kuru-plaque is observed in the molecular layer of the upper vermis of the cerebellum (HE stained; scale bar = 10 μm). (G) Many plaque-type prion protein deposits are seen in the molecular layer of the upper vermis (immunostaining with anti-PrP antibody; scale bar = 50 μm).

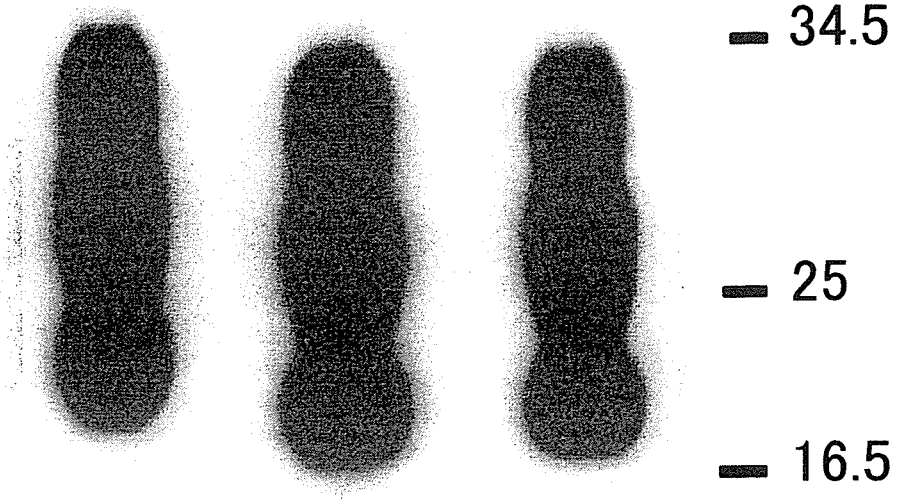

Fig. 3 Western blot analysis of the brain. Left lane: type 1 PrP, Center lane: type 2 PrP (our case), Right lane: another type 2 PrP case.

Table 1 Comparison of pathological features

Pathology	MM2 cortical	MV2	VV2	Our case
Cerebral cortex	○			○
Basal ganglia/thalamus		○		
Cerebellum			○	○
Kuru plaque		○		○
Plaque-like PrP deposit		○	○	○
Coarse perivacuolar PrP deposit	○			○

○ indicates constantly observed pathological findings.

ACKNOWLEDGMENTS

The authors thank Katsumi Doh-ura, Department of Neurological Science, Tohoku University Graduate School of Medicine, for his assistance in the analysis of CSF.

This study was partly supported by a grant from the Research Committee on Prion Disease and Slow Virus Infection, Ministry of Health, Welfare, and Labor, Japan.

REFERENCES

1. Parchi P, Giese A, Capellani S *et al.* Classification of sporadic Creutzfeldt-Jakob disease based on molecular and phenotypic analysis of 300 subjects. *Ann Neurol* 1999; **46**: 224–233.
2. Kitamoto T, Shin RW, Doh-ura K *et al.* Abnormal isoform of prion protein accumulates in the synaptic structures of the central nervous system in patients with Creutzfeldt-Jakob disease. *Am J Pathol* 1992; **140**: 1285–1294.
3. Shimizu S, Hoshi K, Muramoto T *et al.* Creutzfeldt-Jakob disease with florid-type plaques after cadaveric dura mater grafting. *Arch Neurol* 1999; **56**: 357–362.
4. Zerr I, Schulz-Schaeffer WJ, Giese A *et al.* Current clinical diagnosis in Creutzfeldt-Jakob disease: identification of uncommon variants. *Ann Neurol* 2000; **48**: 323–329.
5. Meissner B, Köhler K, Körtner K *et al.* Sporadic Creutzfeldt-Jakob disease. Magnetic resonance imaging and clinical findings. *Neurology* 2004; **63**: 450–456.
6. Hamaguchi T, Kitamoto T, Sato T *et al.* Clinical diagnosis of MM2-type sporadic Creutzfeldt-Jakob disease. *Neurology* 2005; **64**: 643–648.
7. Samman I, Schulz-Schaeffer WJ, Wöhrle JC *et al.* Clinical range and MRI in Creutzfeldt-Jakob disease with heterozygosity at codon 129 and prion protein type 2. *J Neurol Neurosurg Psychiatry* 1999; **67**: 678–681.

Neuropathology 2006; **26**, 447–454

doi:10.1111/j.1440-1789.2006.00717.x

Case Report

An autopsy case of frontotemporal dementia with severe dysarthria and motor neuron disease showing numerous basophilic inclusions

Kenji Ishihara,[1,2] Shigeo Araki,[3] Nami Ihori,[4] Jun-ichi Shiota,[1,2] Mitsuru Kawamura[1] and Imaharu Nakano[5]

[1]Department of Neurology, Showa University School of Medicine, Tokyo, [2]Department of Neurology, Ushioda General Hospital, Yokohama, Departments of [3]Neurology and [4]Rehabilitation, Kawasaki Cooperation Hospital, Kanagawa, and [5]Department of Neurology, Jichi Medical School, Tochigi, Japan

We report a clinicopathological study of a patient suffering from frontotemporal dementia (FTD) with severe dysarthria and concomitant motor neuron disease (MND). The patient was a 52-year-old woman with almost simultaneous emergence of severe dysarthria and FTD. The severe dysarthria subsequently evolved into anterior opercular syndrome. Motor neuron signs then emerged, and the patient developed akinetic mutism approximately 2 years after the onset of the disease. The patient died of pneumonia after a 7-year clinical illness. Pathologically, severe and widespread degeneration in the frontal and temporal lobes, including the anterior opercular area, limbic system, basal ganglia, spinal cord and cerebellum, and frequent ubiquitin- and tau-negative basophilic inclusions were observed. The pyramidal tracts and anterior horns of the cervical cord also showed marked degeneration. Cases showing basophilic inclusions reported so far have been divided into two groups: early onset FTD and MND with basophilic inclusions. Our case presented clinicopathological features of both FTD and MND, which suggests that cases showing basophilic inclusions may constitute a clinicopathological entity of FTD/MND.

Key words: anterior opercular syndrome, basophilic inclusion, frontotemporal dementia, motor neuron disease, Pick's disease.

INTRODUCTION

Although mutism is a late symptom of frontotemporal dementia (FTD), disordered speech is usually not observed in the early stages.[1] On the other hand, in FTD with motor neuron disease (FTD/MND), which is a subgroup of FTD, severe dysarthria attributable to bulbar palsy is observed within approximately 6 months to 1 year after the onset of the disease.[1,2] This subgroup shows a rapid progression to akinetic mutism, and most patients die within 3 years of the disease onset. The pathological hallmarks of FTD/MND are ubiquitin-positive intraneuronal inclusions in the cortical layer II of the frontal and temporal cortices and granule cells in the hippocampal dentate gyrus,[2–4] and focal degeneration of the rostral CA1-subiculum border.[5]

We report an autopsied case of FTD with MND that showed severe dysarthria in the early stage and a rapid progression to akinetic mutism but was pathologically different from FTD/MND, because this case lacked ubiquitin-positive inclusions but showed numerous ubiquitin-negative basophilic inclusions in the widespread lesions in the central nervous system.

CASE REPORT

Clinical summary

A 52-year-old right-handed Japanese woman visited our hospital because of speech difficulties. Around this time, the patient's activity level decreased, and she became disinterested in performing activities of daily living, such as cooking and washing clothes. Her medical history was unremarkable except for chronic thyroiditis, and she had

Correspondence: Kenji Ishihara, MD, Department of Neurology, Showa University School of Medicine, Hatanodai 1-5-8, Shinagawa-ku, Tokyo 142-8666, Japan. Email: k-ishihara@mvj.biglobe.ne.jp

Received 14 November 2005; revised and accepted 3 February 2006.

no family history of neurological diseases. At the clinic, her voice was weak, hoarse and coarse owing to prominent breath sounds, and her speech duration time was short. The movements of her speech organs (tongue, jaw, soft palate and cheek) were not limited in range, but were slow. Spontaneous speech was not substantially distorted, but was monotonous with impaired prosody. Singing was also disturbed. Although she was able to understand oral and written language, she had mild attention deficit and cognitive impairment. She scored a verbal IQ 68, performance IQ 62 and full-scale IQ 61 on the revised edition of the Wechsler adult intelligence scale. She was aware of her difficulty in speech.

The patient was admitted to our hospital approximately 1 year later because her speech had deteriorated. On admission, her general condition was unremarkable. She was apathetic with poor facial expression and paid no attention to her surroundings. She was almost mute and unconcerned with her clothes or appearance. Only occasionally her speech was so nasal and monotonous that the vowels and consonants were too distorted to be comprehended. In addition, her voice was severely hoarse and coarse, with prominent breath sounds. The patient could not sing, and she had no forced crying or laughter. There was no wasting or fasciculation of the tongue, but movements of the speech organs were disturbed. She could not intentionally move the facial muscles, tongue or soft palate, but she could open her mouth naturally while yawning, and her tongue moved sufficiently at meals (automatico-voluntary dissociation). The results of a nasolaryngoscopy showed normal symmetrical movements of the vocal cords. The limb muscle tone was normal. The tendon reflexes were within normal range, and pathological reflexes were not observed. Based on these clinical findings, we made a diagnosis of progressive anterior opercular syndrome (AOS).

Routine laboratory examinations did not show any abnormalities, such as thyroid dysfunction, syphilis or vitamin deficiencies. A brain MRI showed bilateral enlargement of the anterior horn of the lateral ventricles (Fig. 1).

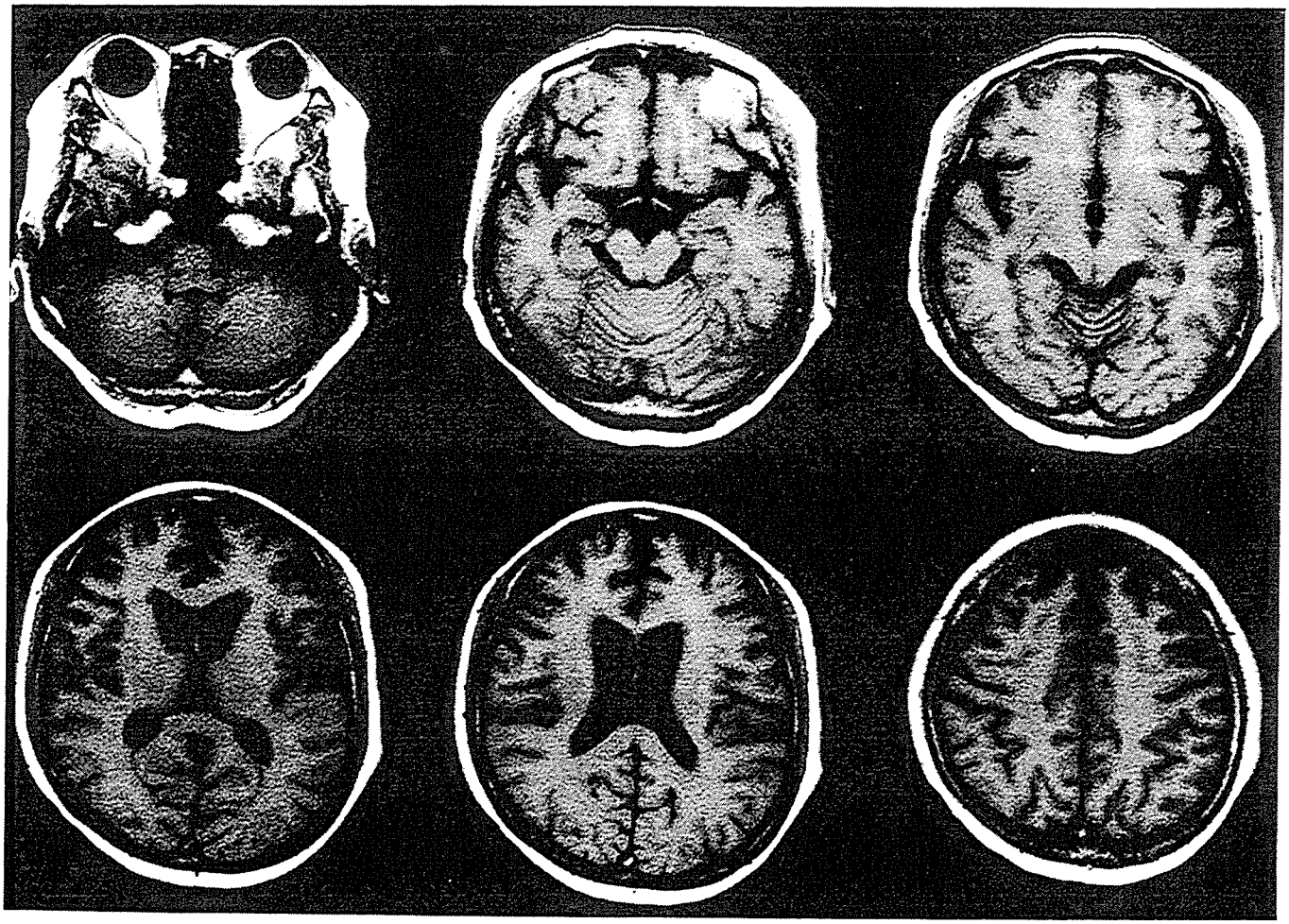

Fig. 1 MRI performed on the first admission. The anterior horns of the bilateral lateral ventricles are enlarged, suggesting atrophy of the caudate head.

The SPECT image showed hypoperfusion in the frontotemporal cortex and subcortical area bilaterally. The EEG did not show any abnormality.

After she was discharged, the patient repeatedly went to the toilet but did not urinate or defecate. She aimlessly wandered in her house and frequently fell. At meals, she continuously brought food to her mouth without swallowing, and her behavior had to be monitored by her family all day.

Six months later, she was readmitted because of exacerbated neurological conditions. She had bilateral pyramidal tract signs (brisk tendon reflexes, spasticity in the lower limbs and positive Babinski's sign), extrapyramidal symptoms (akinesia and postural instability), and frontal lobe signs (palmomental reflexes and snout reflexes). She showed stereotypical behaviors. For example, she repeatedly brought an empty cup to her mouth and mimicked drinking water; she also aimlessly repeated standing up and sitting down on the bed. A brain MRI showed a rapid progression of atrophy in the bilateral frontal-temporal lobes (Fig. 2). Electromyography performed in the right hand and leg showed neurogenic changes, suggesting anterior horn cell degeneration. A feeding tube was eventually inserted due to her difficulty with swallowing.

Approximately 2 years after the onset of the disease, the patient developed akinetic mutism and quadriparesis. She died of pneumonia about 7.5 years after the initial manifestation of the speech disorder. The clinical diagnosis was FTD/MND presenting with progressive AOS in the early stage.

Pathological findings

Pathological examination was performed only on the brain. Paraffin-embedded sections obtained from the appropriate regions of the cerebrum, brainstem, cerebellum and spinal cord were stained with HE, Klüver-Barrera's, Bodian's and Nissl stains. Immunostaining using

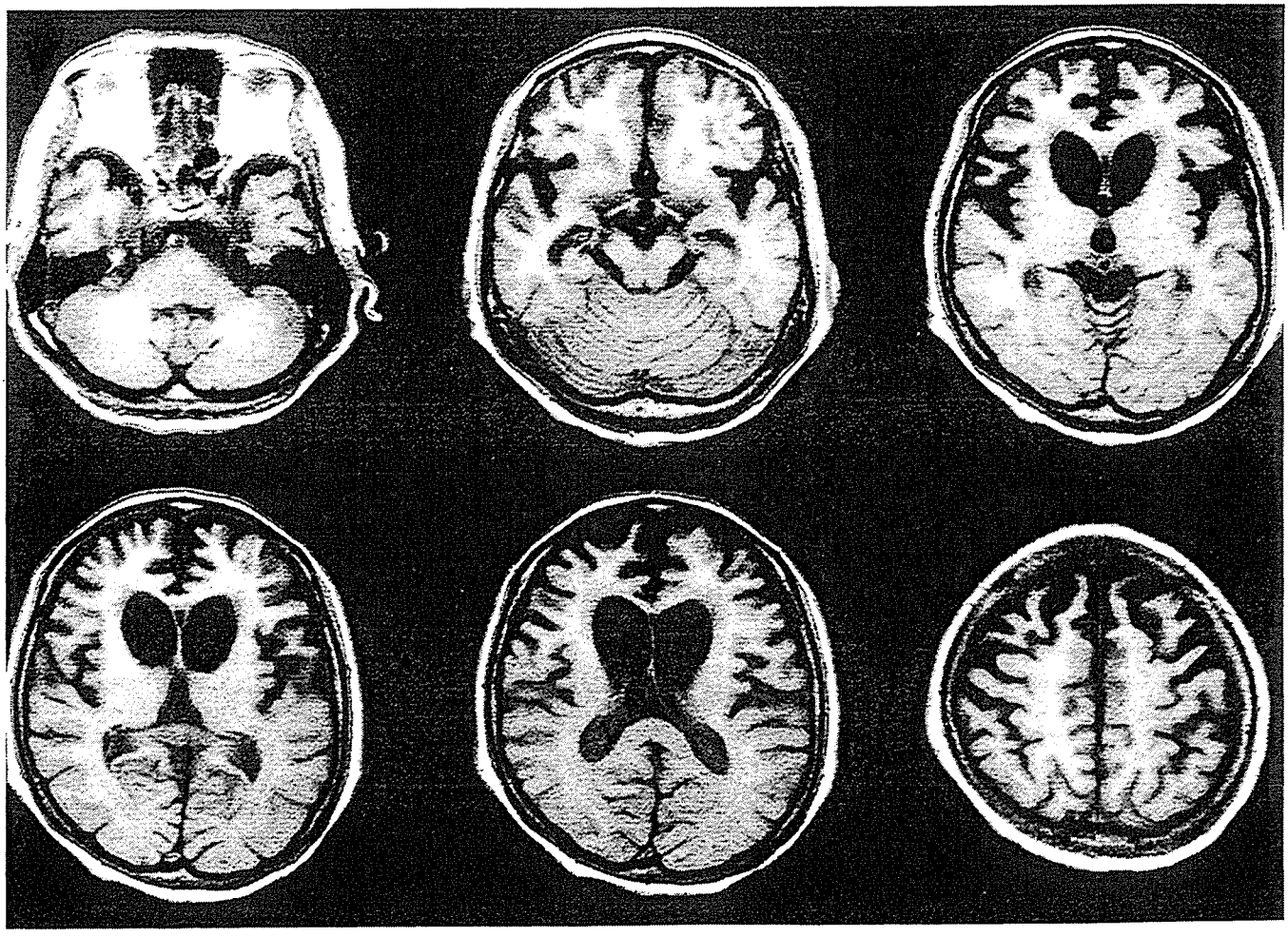

Fig. 2 MRI performed about 1 year after the first admission. Prominent atrophy of the bilateral frontal and anterior temporal lobes can be seen.

antitau (AT8; Innogenetics, Ghent, Belgium; 1:1000), antiubiquitin (Dako; Glostrup, Denmark; 1:100) and antialpha-synuclein (monoclonal; LB509; 1:100) antibodies was also performed in some sliced sections.

The fixed brain weighed 710 g. Macroscopically, severe atrophy of the bilateral frontal and anterior temporal lobes involving the precentral gyrus was observed (Fig. 3), while the parietal and occipital lobes were preserved in volume. The brainstem was atrophic. The medial two-thirds of the cerebral peduncle showed prominent brownish discoloration. The coronal sections of the cerebrum showed prominent enlargement of the lateral ventricles and severe atrophy of the bilateral frontal and anterior temporal lobes and the limbic system (Fig. 3). The cortex in these lobes was thin, and the volume of the white matter was reduced. The deeply located structures were also degenerated to the point that the caudate nucleus, putamen, globus pallidus, subthalamic nucleus and thalamus were difficult to recognize separately. The horizontal sections of the brainstem and cerebellum showed severe atrophy of the brainstem. The bilateral pyramids were also atrophic.

Histopathological examination showed severe and diffuse neuronal loss, gliosis and rarefaction of the neuropil in the frontal and temporal lobes, the hippocampus, amygdala, basal ganglia, thalamus and substantia nigra (Fig. 4). In contrast, the cerebral cortices in the parietal and occipital lobes were preserved. There were numerous basophilic inclusions in the frontal and temporal lobes, limbic systems, basal ganglia, subthalamic nucleus, nucleus basalis of Meynert, red nucleus, substantia nigra, locus ceruleus, pontine nucleus, inferior olivary nucleus and anterior horn of the higher cervical cord (Fig. 5). The basophilic inclusions were weakly argyrophilic and stained with Nissl stain, but were not stained with antitau (AT-8), antiubiquitin or antialpha-synuclein antibodies. Neurofibrillary tangles or senile plaques were scarcely observed even in their preferential areas. In the cerebellum, several basophilic inclusions in the neurons of the dentate nucleus, loss of Purkinje cells and many torpedoes were observed. Pallor of the myelin sheath and severe reduction of the myelinated nerve fibers in the pyramidal tracts, at the level of cerebral peduncle, medullary pyramids and higher cervical cord were observed (Fig. 6). Motor neurons in the facial and hypoglossal nucleus and high cervical anterior horns were obviously reduced in number. The intramedullary roots of the hypoglossal nerve showed degeneration. How-

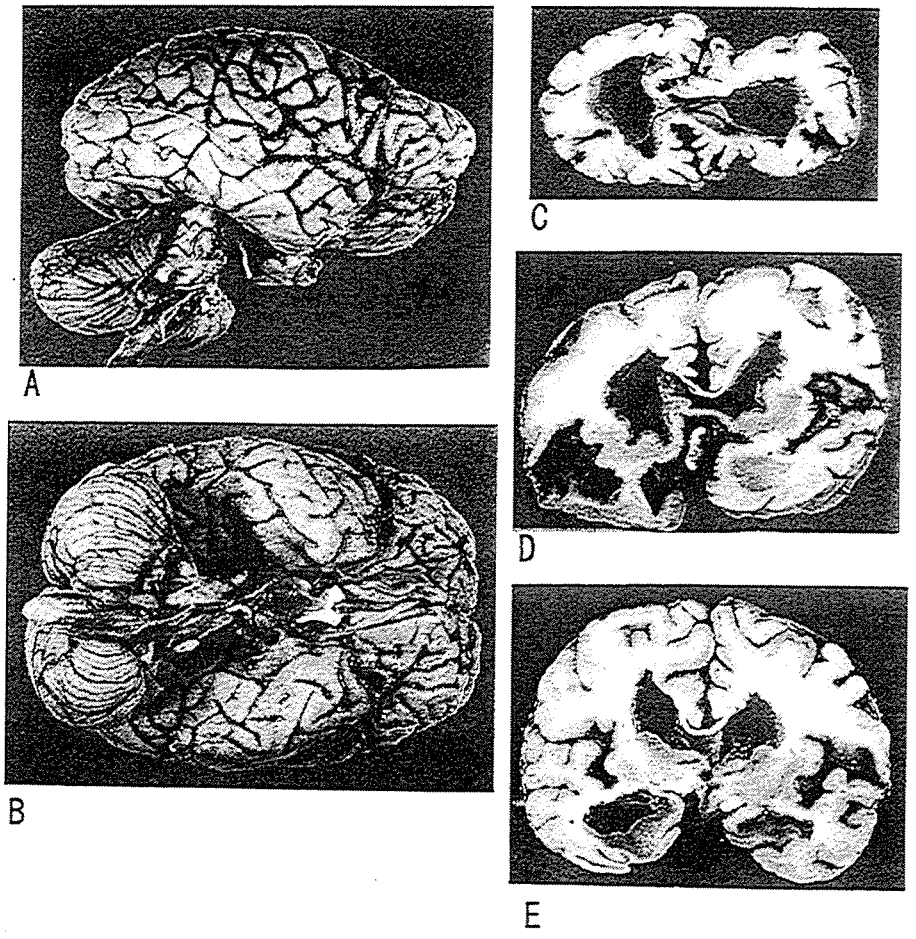

Fig. 3 Macroscopic appearance of the fixed brain. (A,B) Severe atrophy of the frontal lobes, including the precentral gyrus, anterior temporal lobes, and the brain stem, can be seen. (C,D,E) In the coronal sections, prominent enlargement of the lateral ventricles and severe atrophy of the bilateral frontal and anterior temporal lobes and the limbic system can be seen. (A) Lateral view from the right side. (B) Basal surface of the brain and brain stem. Coronal sections through the (C) genu of the corpus callosum, (D) amygdala and (E) hippocampus.

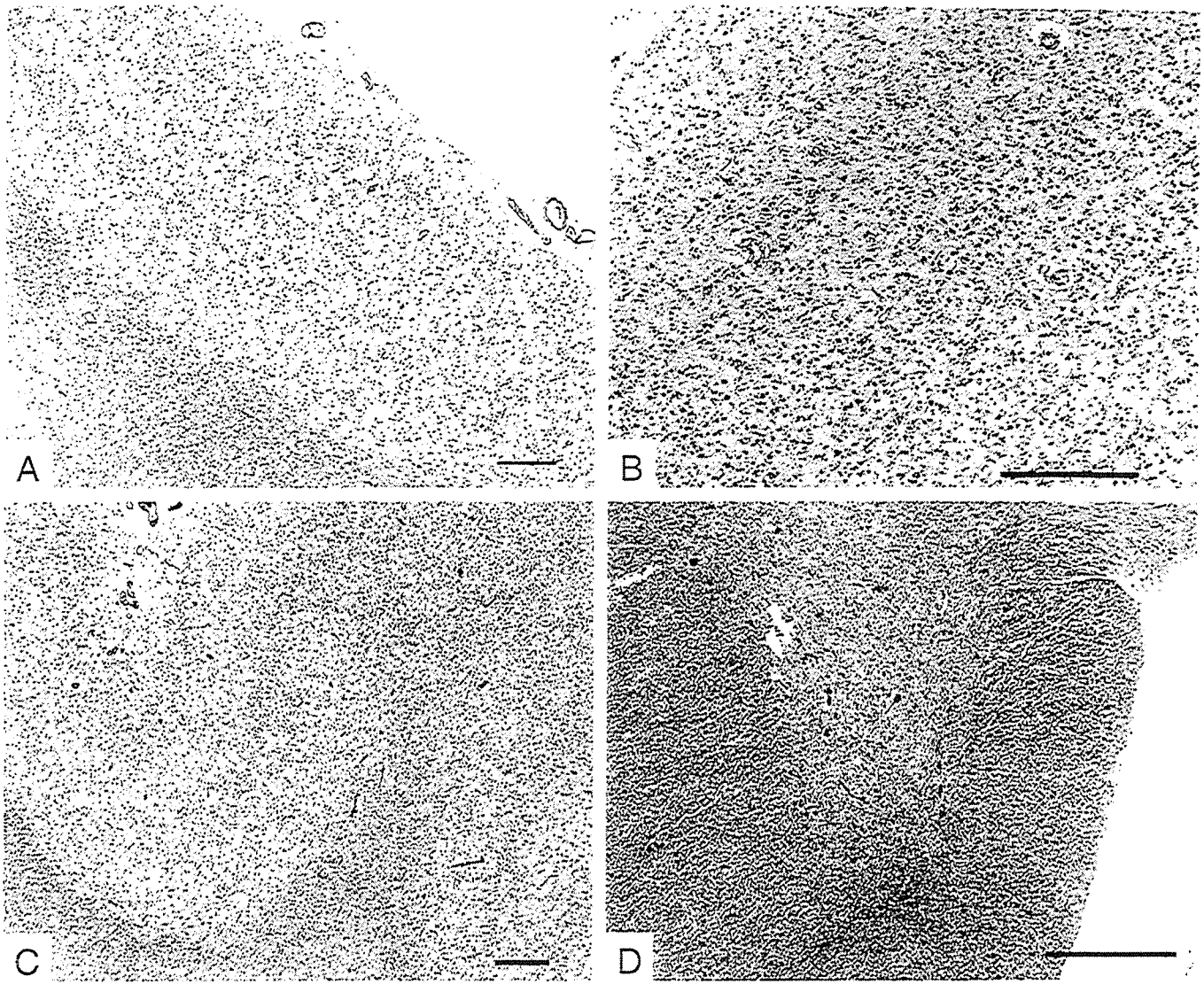

Fig. 4 Microscopic findings. (A–C) Severe neuronal loss, gliosis, and rarefaction of the neuropil can be seen. (A) Frontal lobe (HE; bar = 200 μm). (B) Precentral gyrus (HE; bar = 200 μm). (C) Temporal lobe (HE; bar = 400 μm). (D) Motor neurons in the anterior horn of the cervical cord are markedly reduced in number (HE; bar = 200 μm).

ever, there were no Bunina bodies or ubiquitin-positive intraneuronal inclusions.

DISCUSSION

The early decline in social interpersonal conduct, decline in personal hygiene and grooming, perseverative and stereotypical behaviors, and late mutism observed in the presented case are clinical features of FTD.[1,6] The bilateral pyramidal tract signs and neurogenic findings in EMG observed in the middle stage support the clinical diagnosis of MND. Therefore, with the rapid progression into akinetic mutism, this case is clinically compatible with FTD/MND.

The dysarthria observed in the initial stage was characterized by hoarseness, followed by the emergence of a nasal voice and volitional movement disorders of the speech organs, which ultimately evolved into AOS. MND signs, such as tongue atrophy and fasciculation, were not observed even in this stage; therefore, the severe dysarthria was thought to be attributable to AOS, not bulbar palsy. This is a unique clinical feature of our case because severe dysarthria is caused by bulbar palsy in FTD/MND.[1] Progressive AOS is a rare condition,[7] and to the best of our knowledge, no other case of progressive AOS with FTD has been reported in the literature. We propose that the combination of FTD and progressive AOS in our case was derived from severe and widespread lesions in the bilateral

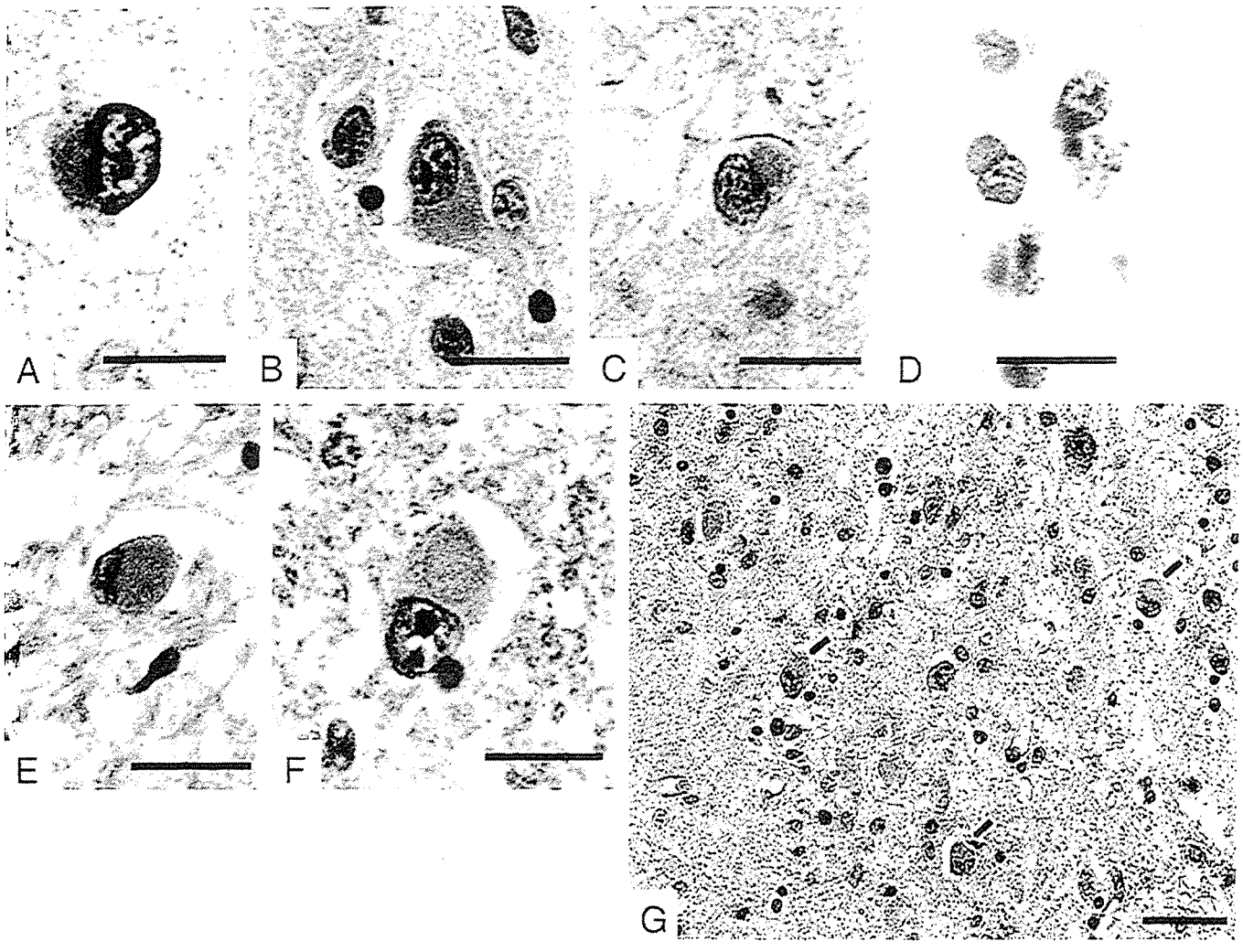

Fig. 5 Basophilic inclusion bodies observed in the brain. (A) Frontal lobe (HE; bar = 10 μm). (B) Temporal cortex (HE; bar = 20 μm). (C) Precentral gyrus (HE; bar = 20 μm). (D) Insular cortex (KB; bar = 20 μm. (E) Subthalamic nucleus (HE; bar = 20 μm). (F) Red nucleus (HE; bar = 10 μm). (G) Hippocampus, basophilic inclusions are indicated by arrows (HE; bar = 20 μm).

frontal lobes, including the anterior opercular area, which is supported by the SPECT and pathological findings.

Intraneuronal inclusions observed in the present case were basophilic with HE and KB stain, well stained with Nissl stain, weakly argyrophilic with Bodian's stain, and negative with AT8 and antiubiquitin immunostaining. Although electromicroscopic examination was not performed, these findings coincide well with a previous report of basophilic inclusions.[8] Basophilic inclusions have been described in cases of juvenile onset amyotrophic lateral sclerosis.[9–13] So far, adult-onset cases showing basophilic inclusions consist of two major subgroups:[14] one is a generalized variant of Pick's disease or relatively early onset FTD,[15] and the other is motor neuron disease with basophilic inclusions. Although only a few cases in each subgroup have been reported,[8,15–18] some of these cases show a widespread distribution of lesions as was observed in our case.

The present case showed clinicopathological features of both FTD and MND, which suggests that cases showing basophilic inclusions may constitute a clinicopathological spectrum of FTD/MND between a generalized variant of Pick's disease (FTD) and motor neuron disease with basophilic inclusions (MND). This condition clinically mimics FTD/MND with ubiquitin-positive inclusions, but differs pathologically.

ACKNOWLEDGMENTS

This study was supported by Showa University Grant-in-Aid for Innovative Collaborative Research Projects, Core Research for Evolutional Science and Technology

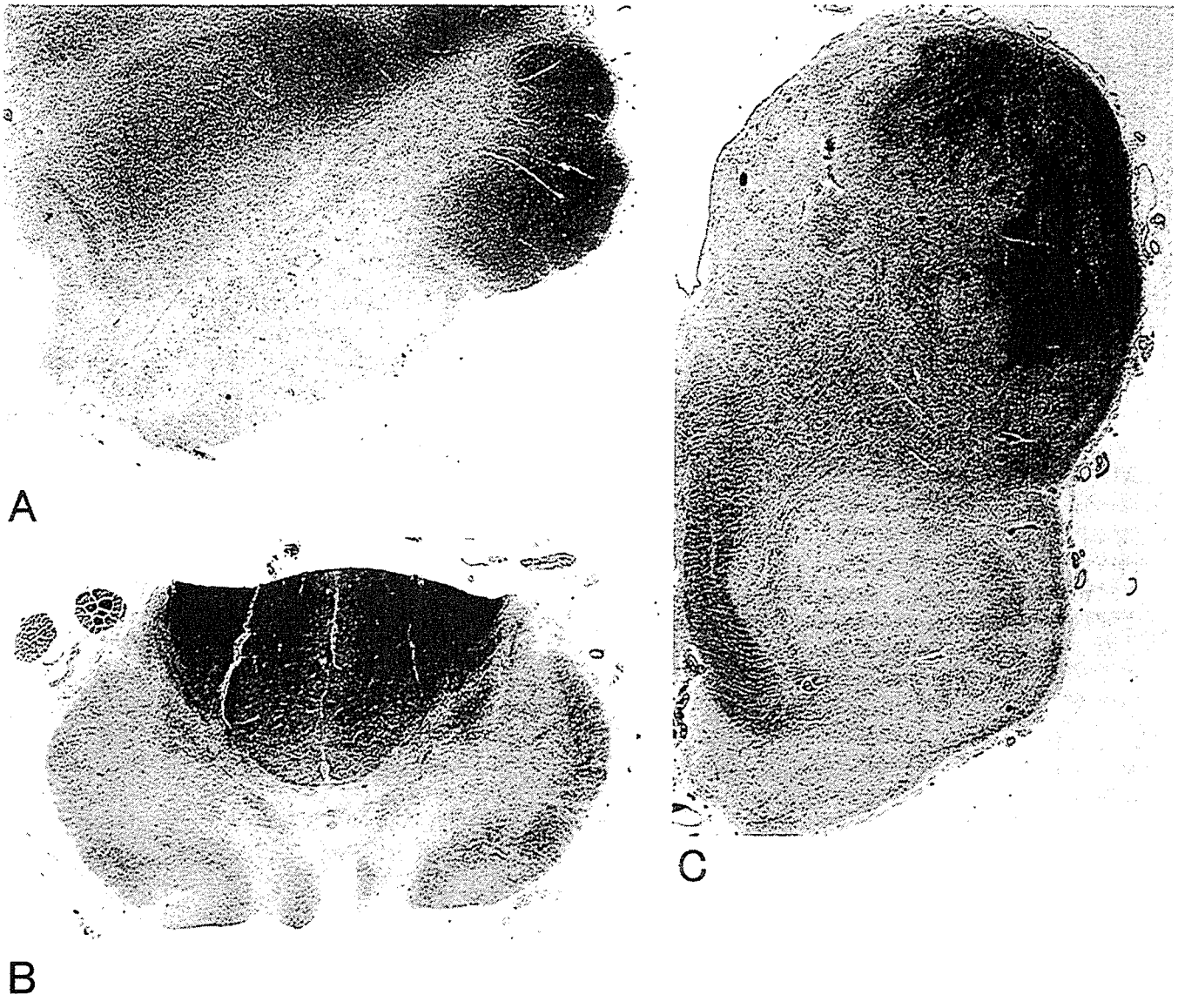

Fig. 6 Semimacroscopic findings of the brainstem and cervical cord. (A) Cerebral peduncle (KB). (B) Medulla oblongata (KB). (C) Upper cervical cord (KB). Prominent pallor of the myelin sheath of the corticospinal tract can be seen.

(CREST), and a Grant-in-Aid for Scientific Research on Priority Areas (17022035) from the Japanese Ministry of Education, Culture, Sports, Science and Technology.

REFERENCES

1. Snowden J, Neary D, Mann DMA. *Fronto-Temporal Lobar Degeneration: Frontotemporal Dementia, Progressive Aphasia, Semantic Dementia.* New York: Churchill Livingstone, 1996.
2. Bak TH, Hodges JR. Motor neurone disease, dementia and aphasia: coincidence, co-occurrence or continuum? *J Neurol* 2001; **248**: 260–270.
3. Jackson M, Lowe J. The new neuropathology of degenerative frontotemporal dementias. *Acta Neuropathol* 1996; **91**: 127–134.
4. Tolnay T, Probst A. Frontotemporal lobar degeneration. An update on clinical, pathological and genetic findings. *Gerontology* 2001; **47**: 1–8.
5. Nakano I. Frontotemporal dementia with motor neuron disease (amyotrophic lateral sclerosis with dementia). *Neuropathology* 2000; **20**: 68–75.
6. Neary D, Snowden JS, Gustafson L *et al.* Frontotemporal lobar degeneration. A consensus on clinical diagnostic criteria. *Neurology* 1998; **51**: 1546–1554.
7. Weller M. Anterior opercular cortex lesions cause dissociated lower cranial nerve palsies and anarthria but

no aphasia: Foix–Chavany–Marie syndrome and 'automatic voluntary dissociation' revisited. *J Neurol* 1993; **240**: 199–208.
8. Kusaka H, Matsumoto S, Imai T. Adult-onset motor neuron disease with basophilic intraneuronal inclusion bodies. *Clin Neuropathol* 1993; **12**: 215–218.
9. Wohlfart G, Swank RL. Pathology of amyotrophic lateral sclerosis. Fiber analysis of the ventral root and pyramidal tracts of the spinal cord. *Arch Neurol Psychiatry* 1941; **46**: 783–799.
10. Berry RG, Chambers RA, Duckett S *et al.* Clinicopathological study of juvenile amyotrophic lateral sclerosis. *Neurology* 1969; **19**: 312.
11. Nelson JS, Prensky AL. Sporadic juvenile amyotrophic lateral sclerosis. A clinicopathological study of a case with neuronal cytoplasmic inclusions containing RNA. *Arch Neurol* 1972; **27**: 300–306.
12. Oda M, Akagawa N, Tabuchi Y *et al.* A sporadic juvenile case of the amyotrophic lateral sclerosis with neuronal intracytoplasmic inclusions. *Acta Neuropathol* 1978; **44**: 211–216.
13. Matsumoto S, Kusaka H, Murakami N *et al.* Basophilic inclusions in sporadic juvenile amyotrophic lateral sclerosis: an immunocytochemical and ultrastructural study. *Acta Neuropathol* 1992; **83**: 579–583.
14. Munoz DG. The pathology of Pick complex. In: Kertesz A, Munoz DG (eds) *Pick's Disease and Pick Complex*. New York: Wiley-Liss, 1998; 211–241.
15. Munoz-Garcia D, Ludwin SK. Classic and generalized variants of Pick's disease: a clinicopathological, ultrastructural and immunocytochemical comparative study. *Ann Neurol* 1984; **16**: 467–480.
16. Kusaka H, Matsumoto S, Imai T. An adult-onset case of sporadic motor neuron disease with basophilic inclusions. *Acta Neuropathol* 1990; **80**: 660–665.
17. Hamada K, Fukazawa T, Yanagihara T *et al.* Dementia with ALS features and diffuse Pick body-like inclusions (atypical Pick's disease?). *Clin Neuropathol* 1995; **14**: 1–6.
18. Tsuchiya K, Ishizu H, Nakao I *et al.* Distribution of basal ganglia lesions in generalized variant of Pick's disease: a clinicopathological study of four autopsy cases. *Acta Neuropathol* 2001; **102**: 441–448.

Prevention of diabetic retinopathy by intraocular soluble *flt-1* gene transfer in a spontaneously diabetic rat model

JUNICHI IDENO[1,2], HIROAKI MIZUKAMI[1], AKIHIRO KAKEHASHI[3], YUKA SAITO[3], TAKASHI OKADA[1], MASASHI URABE[1], AKIHIRO KUME[1], MASATOSHI KUROKI[4], MASANOBU KAWAKAMI[4], SHUN ISHIBASHI[2] and KEIYA OZAWA[1]

[1]Division of Genetic Therapeutics, Center for Molecular Medicine, [2]Department of Medicine, Division of Endocrinology and Metabolism, Jichi Medical University, Tochigi, Japan; [3]Department of Ophthalmology, [4]Department of Comprehensive Medicine I, Omiya Medical Center, Jichi Medical University, Saitama, Japan

Received August 11, 2006; Accepted October 2, 2006

Abstract. The number of patients suffering from diabetes mellitus is constantly rising worldwide, and diabetic retinopathy (DR) has become the most frequent cause of postnatal blindness. Vascular endothelial growth factor (VEGF) is known to play a central role during DR development. Thus, inhibiting the effects of VEGF may hamper the disease progression, and gene transfer of the soluble VEGF receptor *sflt-1* is an attractive approach for this purpose. However, the lack of suitable animal models hindered the evaluation of this strategy. Recently, the spontaneously diabetic non-obese Torii (SDT) rat was established and is considered as one of the ideal models for human DR. In this study, we evaluated the efficacy of gene therapy in SDT rats by using adeno-associated viral vectors (AAV-*sflt-1*) injected into the subretinal space. Thirty weeks later, the progression of DR was assessed by fluorescein angiography using three parameters; the presence of an avascular area, extensive hyperfluorescein and arterial narrowing. These changes were significantly less evident in the 'treated' eyes than in the control. No adverse effects were observed throughout the study. These results indicate that local *sflt-1* gene transfer inhibits DR progression in SDT rats and offers powerful therapeutic potential for the management of human DR.

Introduction

Diabetic retinopathy (DR) is one of the major complications of diabetes mellitus (DM), and the most frequent cause of postnatal blindness (1,2). The number of patients suffering from DM is steadily increasing worldwide (3), and the prevention of DR has become a matter of great importance. Unfortunately, the number of patients who are losing their vision due to DR is increasing despite the technological advancements, especially laser photocoagulation and vitreous surgery. Therefore, the development of a novel therapeutic approach to prevent DR progression has a vital significance.

Proliferative diabetic retinopathy (PDR) is an advanced form of DR characterized by neovascularization, vitreous hemorrhage and tractional retinal detachment. Although a number of biochemical changes, including increased polyol pathway activity (4,5), activation of protein kinase C (6-8) and accumulation of advanced glycation end-products (9,10) were reported in the development of PDR, vascular endothelial growth factor (VEGF), a potent endothelial cell-specific mitogen, plays a critical role in the angiogenesis of PDR (11-13). The actions of VEGF are mediated by the fms-like receptors, Flt-1 and Flk-1/KDR, which are expressed on vascular endothelial cells, and result in endothelial cell proliferation, migration, and increased vasopermeability with tyrosine kinase activity (14-17). Expression of VEGF is upregulated by hypoxia, and increased vitreous VEGF levels were observed in patients with PDR (12,18,19). Moreover, overexpression of VEGF by photo-receptors in transgenic mice promoted retinal neovascular-ization (20), whereas antagonists for VEGF suppressed neovascularization in the retina and iris (13,21,22). A soluble form of the VEGF receptor Flt-1 (sFlt-1) is the only known endogenous specific inhibitor for VEGF, and has drawn considerable attention for its potential clinical application in the inhibition of angiogenesis (23-28). It lacks the immuno-globulin-like domain, the transmembrane spanning region and the intracellular tyrosine-kinase domain. The anti-angiogenic activity of sFlt-1 results from the inhibition of VEGF by two mechanisms; the sequestration of VEGF and the formation of inactive heterodimers with membrane spanning isoforms of the VEGF receptors Flt-1 and KDR (26,29). Studies have shown that the administration of viral vectors encoding *sflt-1* inhibited retinal neovascularization in animal models (30,31). However, the actual merits of sFlt-1 in clinically relevant DR models have not been evaluated.

Correspondence to: Dr Hiroaki Mizukami, Division of Genetic Therapeutics, Center for Molecular Medicine, Jichi Medical University, 3311-1 Yakushiji, Shimotsuke, Tochigi 329-0498, Japan
E-mail: miz@jichi.ac.jp

Key words: diabetic retinopathy, gene therapy, *sflt-1*, spontaneously diabetic non-obese Torii rat, adeno-associated viral vector

Recently, a spontaneously diabetic, non-obese Torii (SDT) rat strain was established from the Sprague-Dawley lineage (32). The animals develop DM at ~20 weeks of age and later manifest DR, which is characterized by tractional retinal detachment, retinal hemorrhage, extensive venous dilatation, extensive hyperfluorescence and a non-perfusion area beyond 55 weeks of age (33). These findings are similar to those found in DR patients; therefore, the SDT rat is one of the best-suited models for studying human DR.

Adeno-associated viral (AAV) vectors are becoming popular in the field of gene therapy because of their safety and long-term effectiveness (34,35). A number of studies have demonstrated the efficacy of ocular gene therapy using AAV vectors (30,36), and vectors derived from serotype 5 (rAAV5) showed the highest utility for retinal gene transfer among serotypes tested (37-39). For this reason, we set out to test the utility of gene therapy on preventing DR in SDT rats using an rAAV5 vector encoding human *sflt-1* (rAAV5-*sflt-1*).

Materials and methods

rAAV vector construction and production. The *sflt-1* cDNA was amplified by PCR from the cDNA library of human umbilical vein endothelial cells (HUVEC). The *in vitro* effect of *sflt-1* expression was confirmed according to a method previously reported (40,41). Briefly, a plasmid was transfected into 293 cells with the Ca-phosphate method, the medium from 293 cells was added at specified dilutions to a 96-well plate containing HUVEC, and the cell density was assessed. An rAAV5 vector encoding *sflt-1* cDNA driven by the human cytomegalovirus (CMV) promoter (rAAV5-CMV-*sflt-1*) was constructed (Fig. 1). rAAV vectors were produced with an adenovirus-free system, and were purified by ultra-centrifugation through an Iodixanol (Axis-Shield PoC AS, Oslo, Norway) gradient followed by dialysis (42,43). The titers of the vector stocks were determined by quantitative dot-blot analysis using a BAS-1500 image analyzer (Fuji Film, Tokyo, Japan).

Animals. All animal experiments were performed in accordance with the standards in the Guide for the Care and Use of Laboratory Animals (NIH publication no. 85-23) and the institutional guidelines. Male SDT rats, provided by the Association for the Spontaneously Diabetic Torii Rat, were used in this study. Standard rodent diet and water were provided *ad libitum*. Casual blood glucose levels were measured by the glucose-oxydase method every four weeks using Glutest A (Sanwa Chemical, Tokyo, Japan). Glycosylated hemoglobin (HbA1c) was measured with a latex agglutination test (SRL, Tokyo, Japan), and plasma sFlt-1 levels were determined using a commercially available ELISA kit (Bender MedSystems, San Bruno, CA) at the end of the study.

Subretinal injection of vector solution. Rats at the age of 27 weeks were anesthetized with an intraperitoneal injection of pentobarbital sodium (1 mg/kg), and 0.4% oxybuprocaine chloride eye drops were used for additional analgesia. All surgical procedures were performed under a surgical microscope. The tip of a 10-mm 39-gauge nylon needle

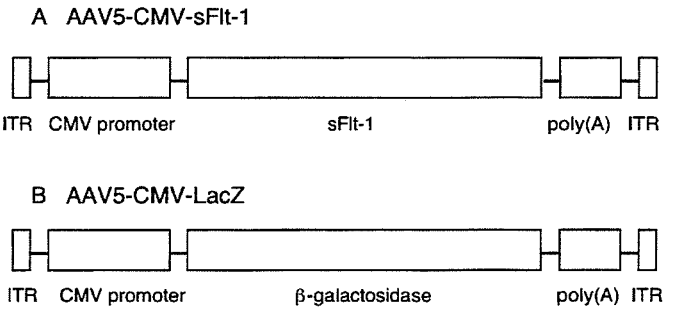

Figure 1. Structure of rAAV vectors. (A) rAAV5-CMV-*sflt-1* vector. (B) rAAV-CMV-*lacZ* vector. ITR, inverted terminal repeat of AAV serotype 5; CMV, human cytomegalovirus promoter; GH, human growth hormone first intron enhancer; Poly (A), SV40 early poly A.

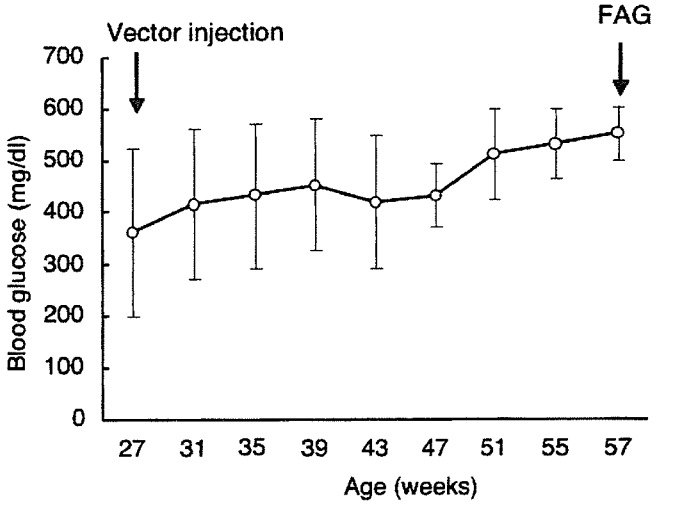

Figure 2. Blood glucose levels of animals during the study. All rats developed diabetes mellitus by the time of subretinal vector administration, and high glucose levels continued throughout the study. Data were shown as mean ± SD, (n=8). FAG, fluorescein angiography.

(Bausch & Lomb, Rochester, NY), mounted on a 10-μl Hamilton syringe, was inserted into the subretinal space through the sclera and ~10 μl of viral suspension was injected. Treated eyes received rAAV5-CMV-*sflt-1* ($4x10^{10}$ vector genome/eye) plus rAAV5 expressing ß-galactosidase (rAAV5-CMV-*lacZ*, $1x10^{10}$ vector genome/eye). Control eyes received only rAAV-CMV-*lacZ* ($1x10^{10}$ viral genome/eye).

Fluorescein-dextran microscopy and quantification of DR. Thirty weeks after the vector administration, the progression of DR was evaluated using fluorescein angiography (FAG). Cardiac perfusion was performed with 1 ml of PBS containing 50 mg of fluorescein-labeled dextran (fluorescein isothiocyanate-dextran; MW, $2x10^6$ daltons; Sigma, St Louis, MO), after administration of a lethal dose of pentobarbital sodium. The eyes were enucleated, the cornea and lens were removed, and the retina dissected from the eyecup. The retina was cut radially and flat-mounted on a glass slide without fixation. A drop of aqueous mounting medium (Crystal/mount, Biomeda

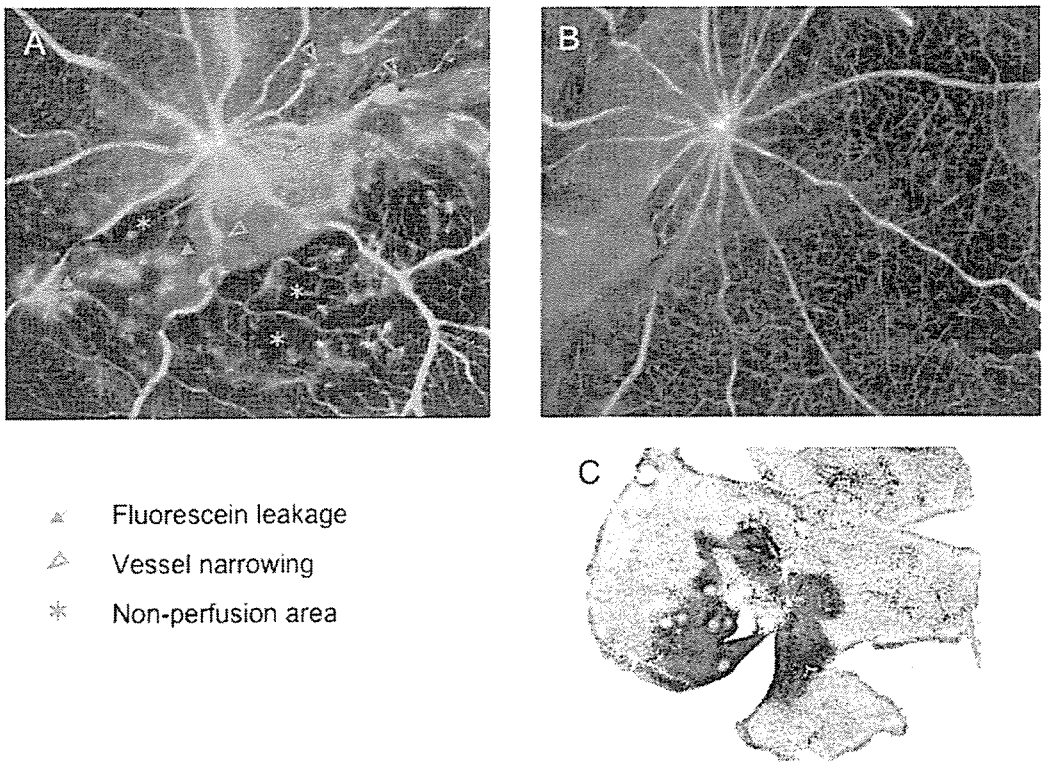

Figure 3. Fluorescein microangiography (FAG) of the rats 30 weeks after vector administration. (A) FAG from AAV5-CMV-*lacZ* injected rats. (B) FAG from rAAV5-CMV-*sflt-1* plus rAAV5-CMV-*lacZ* injected rats. The leakage from the fluorescein spot and avascular area are less extensive in B than in A, thus indicating that the progression of diabetic retinopathy is less marked in the rats treated with rAAV5-CMV-*sflt-1*. (C) A typical X-gal staining of the rat retina showing the distribution of the transduced tissue after subretinal injection of the rAAV-CMV-*lacZ* vector.

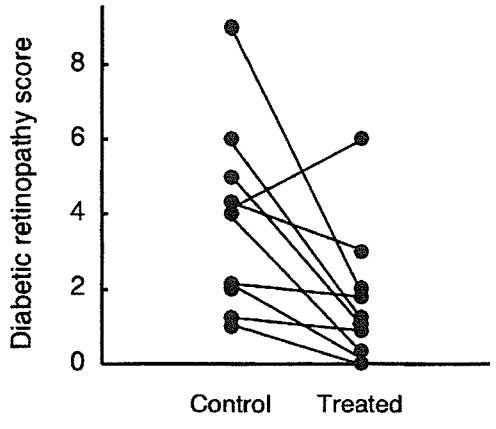

Figure 4. Diabetic retinopathy score of the rats evaluated at the end of the study. The Wilcoxon signed-ranks test demonstrates that the scores for the treated eyes are significantly less than those for the control eyes (n=8, $p<0.05$).

Corp, Foster City, CA) was applied over the retina and allowed to dry. Then the whole flat-mounted retina was examined by fluorescent microscopy (Nikon Labphoto, Nikon, Tokyo, Japan). Without providing information on the vectors injected, the status of DR was determined using the following three parameters: the presence of an avascular area, extensive hyperfluorescence, and arterial narrowing. Each parameter was scored from 0 (none) to 3 (severe) based upon the findings of FAG. The score for each eye was compared and analyzed using the Wilcoxon signed-ranks test. Rats that did not show DR in either of the eyes were excluded from the study. To confirm the subretinal injection of vector solution, X-gal staining of the eye was performed after FAG.

Results

Effect of sFlt-1 in vitro. To prove the biological activity of the protein produced from the *sflt-1* cDNA *in vitro*, we incubated HUVEC with different dilutions of media from 293 cells transfected with the plasmid. The conditioned media from transfected cells inhibited proliferation of HUVEC in a dose-dependent manner, whereas media from untransfected cells had no effect on HUVEC proliferation (data not shown).

Development of DM in SDT rats. All rats developed DM by 35 weeks of age and high blood glucose levels continued throughout the study (Fig. 2). At the end of the study, HbA1c levels in all rats were high (9.4±0.95%; means ± SD), and plasma sFlt-1 was not detected. No adverse effects of sFlt-1 gene therapy were observed throughout the study.

Evaluation of efficacy of gene transfer into the retina. Thirty weeks after the vector administration, FAG was performed to determine the progression of DR. DR was diagnosed using three parameters, arterial narrowing, pooling of fluorescein and a non-perfusion area, and the severity of these parameters were evaluated. The scores of DR in the treated eyes were significantly less than those in the control eyes (Fig. 3A and B; Fig. 4). X-gal staining demonstrated that the LacZ protein was produced in the retinal tissue after transduction with the

rAAV5 vector, and the transgene expression persisted for over 30 weeks after vector administration (Fig. 3C).

Discussion

VEGF is supposedly one of the most essential factors in retinal neovascularization during DR progression. The inhibition of retinal neovascularization by *sflt-1* gene transfer in animal models has been demonstrated in earlier reports (30,31). However, since the mechanisms underlying neovascularization in these models were not related to hyperglycemia, the effectiveness of sFlt-1 in inhibiting DR had not been estimated. To shed light on this issue, a more clinically relevant model has long been awaited. The recently developed SDT rat model is a candidate for this purpose. This model is unique because its diabetic status mimics human NIDDM rather than IDDM. The animals can live for 1 year after the onset of DM without insulin, with a gradual maturation of DR. Therefore, this model is a valuable tool because it can reflect mid- to late-stage human DR associated with NIDDM (32,33). However, this model has certain drawbacks as well. First, the disease progression is much slower than that in other 'conventional' animal models, and DR can be observed mainly after 55 weeks of age. Therefore, one series of experiments requires a long time period. Second, these animals are prone to death, probably due to the complications of DM. Unfortunately, the number of animals decreases before they develop sufficient disease severity. Therefore, to ensure valid results, the sample size of each group needs to be sufficiently large.

This study aimed to demonstrate the efficacy of gene therapy in preventing DR disease progression. For this purpose, we injected the vector soon after the onset of DM, and the efficacy was evaluated at the age of full-blown DR. Considering that a preventive action was significant in this study, a more precise examination of whether short-term *sflt-1* expression is sufficient to prevent DR progression or has an effect in reversing the DR status should be considered for future study. A more difficult task includes determining effective methods to develop this strategy into a clinically realized therapy. Generally, if the therapeutic efficacy is proven in small animals, additional experiments need to be performed on larger animals prior to conducting clinical trials. Regarding DR, no appropriate model has been found in species of large animals. Proliferative DR-like changes were observed in a galactose-fed dog model (44). Nevertheless, this model requires up to 7 years to establish mature DR, which is impractical in a preclinical study. Development of novel large animal models for this purpose is ideal but not practical due to the uncertainty of success in establishing such models during a defined time range. Resolving this problem may not be easy; however, we believe that before clinical trials are considered, further studies using large animals are essential.

In this study, the area of transgene expression was sufficiently wide to protect vision, and the expression continued for over 30 weeks after the injection, indicating that rAAV-mediated ocular gene transfer via a single injection of vector solution could lead to a long-term therapeutic effect. The area of *sflt-1* expression should be comparable to that of X-gal staining, although human sFlt-1 in the retina was undetectable by immunohistochemistry. This may have occurred probably due to technical difficulties in localizing the soluble antigen (31). Therefore, ocular gene transfer under the present experimental conditions is a practical approach. Nonetheless, DR progression was suppressed partially and not completely. At present, it is unclear whether the incomplete suppression was due to the residual actions of VEGF or the uninhibited activity of an alternative angiogenic factor (45). Regarding the latter, a combination of transgenes that act on different aspects of angiogenesis may increase the efficacy of gene therapy for DR prevention.

In patients with DM, VEGF is closely involved in the degree of complication. Elevated VEGF levels in the retina may worsen the DR status and cause visual loss (11,12), while high systemic VEGF levels induce neovascularization, improving ischemic conditions. If circulating sFlt-1 levels affect systemic VEGF levels, DM patients may develop ischemic heart disease, diabetic neuropathy, and diabetic gangrene. To avoid these adverse effects, local sFlt-1 delivery and VEGF inhibition is necessary. In this study, plasma sFlt-1 levels were not elevated after subretinal vector administration, and no adverse effects of *sflt-1* gene transfer were observed. Therefore, the subretinal administration of a vector solution and neutralization of the VEGF activity *in situ* appear to be appropriate measures that should be adopted to achieve our goal.

In conclusion, we demonstrated the successful prevention of DR in SDT rats by using an rAAV vector-encoding *sflt-1* gene. These findings strongly suggest the efficacy of sFlt-1 for DR and the usefulness of rAAV5 for ocular gene transfer. Further studies are necessary to develop and optimize ocular gene therapy for human DR.

Acknowledgements

We thank the Association for the Spontaneously Diabetic Torii Rat for providing the SDT rats. We also thank J.A. Chiorini for providing the systems to produce the AAV5-based vectors. This study was partly supported by grants from the Ministry of Education, Culture, Sports, Science and Technology, and the Ministry of Health, Labor and Welfare, Japan; the 'High-Technology Research Center' Project for Private Universities: a matching fund subsidy from the Ministry of Education, Culture, Sports, Science and Technology, 2003-2007; and the 21st Century Centers of Excellence Program from the Ministry of Education, Culture, Sports, Science and Technology.

References

1. Hyman L: Epidemiology of eye disease in the elderly. Eye 1: 330-341, 1987.
2. Klein BE and Klein R: Ocular problems in older Americans with diabetes. Clin Geriatr Med 6: 827-837, 1990.
3. King H and Rewers M: Global estimates for prevalence of diabetes mellitus and impaired glucose tolerance in adults. WHO *Ad Hoc* Diabetes Reporting Group. Diabetes Care 16: 157-177, 1993.
4. Hotta N, Nakamura J, Sakakibara F, *et al*: Electroretinogram in sucrose-fed diabetic rats treated with an aldose reductase inhibitor or an anticoagulant. Am J Physiol 273: E965-E971, 1997.
5. Robison WG Jr, Nagata M, Tillis TN, Laver N and Kinoshita JH: Aldose reductase and pericyte-endothelial cell contacts in retina and optic nerve. Invest Ophthalmol Vis Sci 30: 2293-2299, 1989.